EGR2 is critical for peripheral naïve T-cell differentiation and the T-cell response to influenza

Ning Du[a], Hyokjoon Kwon[a,1], Peng Li[a], Erin E. West[a], Jangsuk Oh[a], Wei Liao[a], Zuxi Yu[b], Min Ren[a], and Warren J. Leonard[a,2]

[a]Laboratory of Molecular Immunology and Immunology Center, and [b]Pathology Core, National Heart, Lung, and Blood Institute, National Institutes of Health, Bethesda, MD 20892-1674

Edited by Akiko Iwasaki, Howard Hughes Medical Institute, Yale University School of Medicine, New Haven, CT, and accepted by the Editorial Board October 9, 2014 (received for review September 5, 2014)

Early growth response 2 (EGR2) transcription factor negatively regulates T-cell activation, in contrast to the positive regulation of this process by EGR1. Here, we unexpectedly found that EGR2 promotes peripheral naïve T-cell differentiation, with delayed T-cell receptor-induced proliferation in naïve T cells from *Egr2* conditional knockout (CKO) mice and decreased production of IFN-γ, IL-4, IL-9, and IL-17A in cells subjected to T-helper differentiation. Moreover, genes that promote T-cell activation, including *Tbx21* and *Notch1*, had decreased expression in *Egr2* CKO T cells and are direct EGR2 target genes. Following influenza infection, *Egr2* CKO mice had delayed viral clearance, more weight loss, and more severe pathological changes in the lung than did WT and *Egr1* KO mice, with decreased production of effector cytokines, increased infiltration of antigen-specific memory-precursor CD8$^+$ T cells, and lower numbers of lung-resident memory CD8$^+$ T cells. Thus, unexpectedly, EGR2 can function as a positive regulator that is essential for naïve T-cell differentiation and in vivo T-cell responses to a viral infection.

EGR2 | T cells | differentiation | RNA-Seq | influenza

T-cell differentiation involves developmental checkpoints and the actions of multiple transcription factors, including the early growth response (EGR) factors (1). EGR proteins share highly conserved zinc-finger DNA-binding domains that can bind shared target genes (2). In thymocytes, *Egr1*, *Egr2*, and *Egr3* are induced by pre–T-cell receptor (TCR) signaling and promote progression through the β-selection checkpoint (2). *Egr1* is expressed in T cells and thymocytes and acts as a positive regulator for thymocyte development and T-cell activation (3). *Egr2* is critical for hindbrain development and peripheral myelination, with perinatal death in *Egr2* KO mice (4), but it also contributes to T- and B-cell development (5). *Egr2* and *Egr3* are NFAT target genes, and EGR2 induces NFAT-dependent regulation of Fas ligand (6). *Egr2* is implicated in the development of T-cell anergy (7, 8). In CD2-specific *Egr2* conditional knockout (CKO) mice, T cells had normal primary activation but hyperproliferated after prolonged stimulation, and older mice develop a lupus-like syndrome (9), with naïve CD4$^+$ T cells prone to Th1 and particularly Th17 differentiation (10). Moreover, simultaneous deletion of *Egr2* and *Egr3* results in an autoimmune syndrome with increased activated STAT1 and STAT3 but impaired TCR-induced activation of AP-1 (11).

Although studies in vitro and in transgenic mice indicate that EGR2 can negatively regulate T-cell activation and contribute to T-cell anergy, studies of EGR2 in peripheral T-cell differentiation and responses to pathological conditions have been limited. Here, we show that *Egr2* CKO naïve CD4$^+$ and CD8$^+$ T cells had delayed proliferation and impaired Th and Tc cell differentiation, implicating EGR2 as a positive regulator. IL-2 was diminished, a finding we confirmed in WT T cells in which EGR2 was reduced by treatment with siRNA. Moreover, after influenza infection, *Egr2* CKO mice had greater weight loss and pathological changes in their lungs, delayed virus clearance, dysregulated cytokine and chemokine expression, and impaired CD4$^+$ T-cell function with diminished IFN-γ, TNFα, and IL-2. In addition, more of the CD8$^+$ T cells in the lung had a memory phenotype; decreased expression of granzyme B, perforin, IFN-γ, and TNFα; and lower numbers of lung-resident memory CD8$^+$ T cells after long-time infection. In contrast, *Egr1* KO mice were similar to WT mice in their responses. Thus, EGR2 is critical for normal differentiation of naïve T cells and for regulating antigen-specific immune responses to influenza viral infection.

Results

Generating *Egr2* CKO Mice. To investigate the roles of *Egr1* and *Egr2* in T-cell development and function, we obtained *Egr1* KO mice (12) and generated mice in which the entire *Egr2* coding region was floxed (Fig. S1*A*). We used transgenic mice expressing *CD4*-Cre, which deletes the floxed loci at the double-positive (DP) stage in the thymus, thus deleting the *Egr2* coding region in both CD4$^+$ and CD8$^+$ T cells, as we confirmed by PCR (Fig. S1*B*) and Southern blotting (Fig. S1*C*). *Egr2* mRNA expression was essentially absent in splenic T cells stimulated with phorbol 12-myristate 13-acetate (PMA) + ionomycin, whereas neither *Egr1* or *Egr3* expression was significantly altered (Fig. S1*D*); EGR2 protein expression was absent in TCR-stimulated *Egr2* CKO T cells and at an intermediate level in *Egr2*$^{+/f}$*CD4*-Cre$^{+/-}$ cells (Fig. S1*E*).

Analysis of thymocyte subsets revealed modest increases in the percentage of DP cells and decreases in single-positive (SP) cells in *Egr1* KO and *Egr2* CKO mice (Fig. S2*A*). We found increased total thymocytes, double-negative (DN), and DP cells in *Egr1*

Significance

Early growth response 2 (EGR2) is a transcription factor that can negatively regulate T-cell activation. We unexpectedly found that EGR2 promotes peripheral naïve T-cell proliferation and differentiation, with less T-cell receptor-induced IL-2 production in *Egr2*-deficient naïve T cells and diminished cytokine production in T-helper differentiated cells. Moreover, EGR2 was required for T-cell responses to influenza, with delayed viral clearance and more severe pathology in lungs of *Egr2* conditional knockout mice, as well as decreased effector cytokine production from T cells. Thus, EGR2 can act as a positive regulator essential for a normal T-cell response to viral infection, a finding with potential clinical implications.

Author contributions: N.D., H.K., P.L., Z.Y., and W.J.L. designed research; N.D., H.K., P.L., E.E.W., J.O., W.L., Z.Y., and M.R. performed research; N.D., H.K., P.L., Z.Y., and W.J.L. analyzed data; and N.D., H.K., P.L., E.E.W., Z.Y., and W.J.L. wrote the paper.

The authors declare no conflict of interest.

This article is a PNAS Direct Submission. A.I. is a guest editor invited by the Editorial Board.

Data deposition: The data reported in this paper have been deposited in the Gene Expression Omnibus (GEO) database, www.ncbi.nlm.nih.gov/geo (accession no. GSE49366).

[1]Present address: Albert Einstein College of Medicine, Bronx, NY 10461.

[2]To whom correspondence should be addressed. Email: wjl@helix.nih.gov.

This article contains supporting information online at www.pnas.org/lookup/suppl/doi:10.1073/pnas.1417215111/-/DCSupplemental.

KO mice, but no significant changes in *Egr2* CKO mice (Fig. S2*B*). In spleen (Fig. 1*A* and Fig. S2*C*) and lymph nodes (Fig. 1*B* and Fig. S2*D*), deletion of *Egr1* had little effect on peripheral T cells, but *Egr2* CKO mice had fewer $CD3^+$, $CD4^+$, and $CD8^+$ T cells. Although *Egr2* CKO had a slight increase in the percentage of regulatory T (Treg) cells (Fig. S2*E*), the total number of Treg cells was similar to that in WT mice (Fig. S2*F*). B cells, natural killer (NK) cells, $Gr\text{-}1^+Mac\text{-}1^+$ granulocytes, $Mac\text{-}1^+$ monocytes, and $Ter119^+$ erythroid cell numbers were similar in WT, *Egr1* KO, and *Egr2* CKO mice (Fig. S2*G*). There were more $CD44^{hi}/CD62L^{lo}$ $CD4^+$ T cells in *Egr2* CKO than in WT and *Egr1* KO spleens (Fig. 1*C*, *Upper*), consistent with previous reports (9, 13), indicating an increase in effector $CD4^+$ T cells; in contrast, we did not observe an increase in $CD44^{hi}/CD62L^{lo}$ $CD8^+$ T cells in *Egr2* CKO mice (*Lower*).

Defective T-Cell Proliferation and Differentiation in *Egr2* CKO Mice. Because *Egr1* and *Egr2* expression is induced after TCR stimulation (9, 14), we tested the role of EGR1 and EGR2 in T-cell proliferation. After 3-d anti-CD3 + anti-CD28 stimulation, compared with WT naïve cells, *Egr1* KO $CD4^+$ T cells had slightly delayed cell division and *Egr2* CKO $CD4^+$ T-cell division was more delayed (Fig. 2 *A* and *B*). Exogenous IL-2 (100 IU/mL) added during a 3-d TCR stimulation increased proliferation of *Egr2* CKO $CD4^+$ T cells, but not up to the WT level (Fig. 2*A*). Corresponding to this greater responsiveness to IL-2, TCR-stimulated *Egr2* CKO T cells produced less IL-2 than did WT cells; *Egr1* KO T cells had only a slight decrease in IL-2 production that was not statistically significant (Fig. 2*C*). The lower IL-2 production was not anticipated, given reports that EGR2 is needed for anergy (8), but WT $CD4^+$ T cells had a marked decrease in IL-2 production after the introduction of *Egr2* siRNA, confirming that EGR2 is required for normal TCR-induced IL-2 production (Fig. 2*D*). Interestingly, when *Egr2* CKO $CD4^+$ T cells were subjected to Th1, Th2, Th9, and Th17 differentiation, the percentage of cells expressing IFN-γ, IL-4, IL-9, and IL-17A, respectively, was lower than in WT cells (Fig. 2*E*) and ELISA (Fig. 2*F*). In contrast, these cytokines were not significantly decreased in *Egr1* KO $CD4^+$ T cells (Fig. 2 *E* and *F*). The diminished IFN-γ in *Egr2* CKO $CD4^+$ T cells was rescued by exogenous IL-2 (Fig. S3*A*). IL-4 expressing *Egr2* CKO $CD4^+$ T cells were partially increased by exogenous IL-2, but not up to the level of WT cells (Fig. S3*B*), but IL-2 did not increase the percentage of IL-9–expressing cells (Fig. S3*C*). Like *Egr2* CKO $CD4^+$ T cells, *Egr2* CKO $CD8^+$ T cells also had defective proliferation that was partially rescued by exogenous IL-2 (Fig. 2*G*), as well as fewer IFN-γ–expressing cells (Fig. 2*H*) and a modest decrease in IFN-γ production (Fig. 2*I*) that was rescued by exogenous IL-2 (Fig. S3*D*). Such abnormalities were not observed with *Egr1* KO $CD8^+$ T cells (Fig. 2 *G*–*I*).

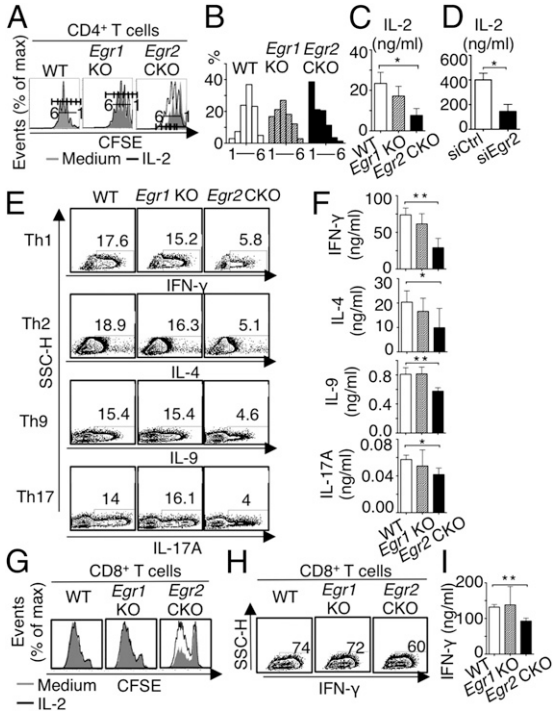

Fig. 2. Defective proliferation and differentiation of naïve $CD4^+$ and $CD8^+$ *Egr2* CKO T cells. (*A*) Naïve splenic and lymph node $CD4^+$ T cells were cultured for 3 d with anti-CD3 + anti-CD28 with or without IL-2, and cell divisions were analyzed by carboxyfluorescein succinimidyl ester (CFSE) dilution and flow cytometry. (*B*) Frequency of CFSE-positive cells at each division. (*C*) After 3-d stimulation, 1×10^6 cells were washed twice in PBS, restimulated with anti-CD3 + anti-CD28 overnight, supernatant was collected, and IL-2 production determined by ELISA. (*D*) IL-2 production by ELISA from WT naïve $CD4^+$ T cells stimulated with TCR for 72 h in the presence of *Egr2* siRNA or control siRNA. (*E*) Naïve $CD4^+$ T cells were differentiated under Th1, Th2, Th9, and Th17 conditions, and indicated cytokines were detected by intracellular staining and flow cytometry. (*F*) After 3-d polarization, 1×10^6 cells were washed twice in PBS, restimulated with anti-CD3 + anti-CD28 overnight, supernatant was collected, and IFN-γ, IL-4, IL-9, and IL-17A were measured by ELISA. (*G*) Analysis of $CD8^+$ T-cell division. (*H* and *I*) Cells were differentiated under Tc conditions and IFN-γ expression was determined by intracellular staining and flow cytometry (*H*) or by ELISA (*I*). Data are from one of four similar experiments with three mice per group in *A*, *B*, *E*, *G*, and *H*, or combined data from three experiments (mean ± SD) in *C*, *F*, and *I*, or representative of three independent experiments in *D*. In *A* and *G*, the shaded area is medium alone, and the black line corresponds to IL-2 treated cells.

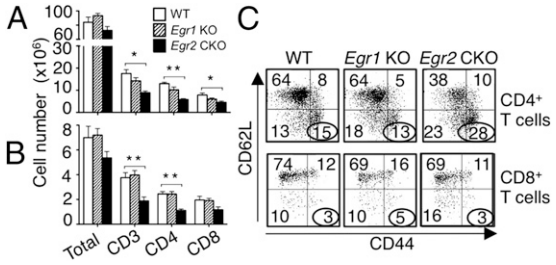

Fig. 1. Decreased T cells in *Egr2* CKO mice. (*A* and *B*) Spleen (*A*) and lymph node (*B*) cells were stained as indicated and analyzed by flow cytometry. Shown are cell numbers from 12 mice per group. (*C*) CD44 and CD62L expression on splenic $CD4^+$ T cells (*Upper*) and $CD8^+$ T cells (*Lower*). Data are from one representative of three experiments with 4 mice per group in each (*C*) and from three experiments (mean ± SD) (*A* and *B*).

Global Analysis of EGR2-Dependent Genes. Using RNA-Sequencing (RNA-Seq), we next compared gene expression profiles in WT and *Egr2* CKO naïve $CD4^+$ T cells that were not stimulated or stimulated with anti-CD3 + anti-CD28 for 1, 4, or 16 h. We identified 1,596, 5,331, and 4,408 genes that were differentially expressed (fold change > 1.5 and P value $< 1 \times 10^{-10}$) between WT and *Egr2* CKO stimulated $CD4^+$ T cells at 1, 4, and 16 h, respectively, with 691, 2,521, and 2,051 induced and 905, 2,810, and 2,357 repressed in *Egr2* CKO T cells (Fig. 3*A* and Dataset S1). Using genes differentially expressed at 16 h, we performed ingenuity pathway analysis (IPA) and identified 134 genes involved in cell development, growth, and differentiation (Fig. 3*B* and Dataset S2*A*). We next focused on genes repressed in *Egr2* CKO T cells and found that some regulated T-cell proliferation and activation (Fig. 3*B*). Interestingly, several transcription factors (e.g., *Notch1*, *Stat5a*, *Tbx21*, and *Gata3*) that promote T-cell

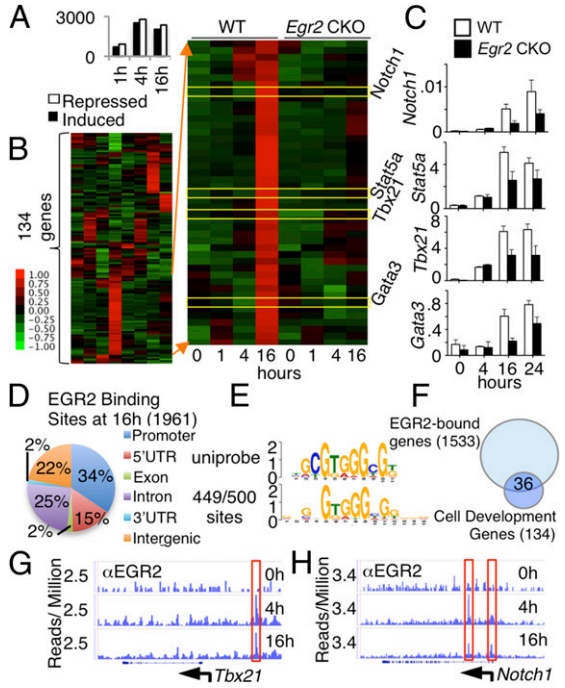

Fig. 3. Gene expression in TCR-induced *Egr2* CKO T cells was altered. (*A–C*) RNA-Seq was performed in WT and *Egr2* CKO naïve CD4$^+$ T cells not stimulated or stimulated with anti-CD3 + anti-CD28 for 1, 4, and 16 h. (*A*) Number of genes induced and repressed in *Egr2* CKO T cells stimulated as indicated (the genes differentially expressed in *Egr2* CKO T cells are listed in Dataset S1). (*B*) Heat map of RNA-Seq data for 134 genes that are differentially expressed (≥1.5-fold difference) in *Egr2* CKO T cells compared with WT T cells (genes are listed in Dataset S2*A*). (*C*) RT-PCR analysis of expression of *Notch1*, *Stat5a*, *Tbx21*, and *Gata3*. (*D*) Genome-wide distribution of EGR2 binding sites based on ChIP-Seq performed in WT T cells not stimulated or stimulated with anti-CD3 + anti-CD28 for 4 and 16 h. The 5′ UTR, 3′ UTR, introns, exons, and intergenic regions were defined according to RefSeq, and promoter regions were defined as regions extending 15 kb 5′ of the transcription start site. Peaks up to 5 kb 3′ of the transcription stop site were considered as binding within the gene body. (*E*) Consensus motif for EGR2. We used TOMTOM to compare the derived motif with the UniPROBE Database. (*F*) The 36 genes related to cell development, growth, and proliferation that exhibited EGR2 binding by ChIP-Seq (genes are listed in Dataset S2*B*). (*G* and *H*) ChIP-Seq analysis of the binding of EGR2 at the *Tbx21* (*G*) and *Notch1* (*H*) loci. Data are representative of two independent experiments.

activation and differentiation (15–18) had lower expression in *Egr2* CKO T cells, as we confirmed by RT-PCR (Fig. 3*C*). To study whether these genes are direct targets of EGR2, we performed ChIP-Seq and identified 1,961 EGR2 binding sites when comparing anti-CD3 plus anti-CD28 stimulated vs. unstimulated WT T cells, after subtracting background IgG control levels, and analyzed EGR2 binding distribution (Fig. 3*D*). To de novo discover EGR2 consensus binding motifs, we used MEME to analyze the top 500 binding sites (sorted by peak *P* value) and found that 449 sites contain a consensus EGR2 motif that is defined in the UniPROBE Database (Fig. 3*E*). Of 134 differentially expressed genes related to cell development, growth, and proliferation (Fig. 3*B*), EGR2 bound to 36 (Fig. 3*F* and Dataset S2*B*), including *Tbx21* (Fig. 3*G*) and *Notch1* (Fig. 3*H*), which had decreased expression in *Egr2* CKO T cells (Fig. 3 *B* and *C*), indicating that *Tbx21* and *Notch1* are direct EGR2 target genes. Thus, EGR2 critically regulates genes that mediate T-cell differentiation and activation. Although EGR2 was shown to bind to the *Dgka* gene under anergic conditions (8), our ChIP-Seq data did not show EGR2 binding at the *Dgka* gene in CD4$^+$ T cells stimulated with anti-CD3 + anti-CD28.

Critical Role for EGR2 in Host Defense to Influenza. Previously, it was reported that EGR2 was not required for normal host responses to lymphocytic choriomeningitis virus (LCMV) or *Toxoplasma gondii* infection (13). To further investigate the role of EGR2 in vivo, we used influenza A viruses, which cause acute respiratory infections in humans and mice. Primary infection of WT mice with influenza strain PR8 results in transient weight loss without overt pathological signs, whereas priming with a serologically distinct strain, X-79, and then infecting mice with PR8 (recall response) results in less severe weight loss than in primary infection, with more rapid recovery to preinfection body weight. *Egr2* CKO mice had progressive weight loss after either primary or recall infection (Fig. 4 *A* and *B*) and had ruffled fur and a hunched posture. Histological examination of lungs from infected *Egr2* CKO mice revealed tissue destruction and lymphocytic infiltration (Fig. 4*C*), with markedly increased pathology scores (Fig. S4*A*). The pathology and body weight changes in *Egr1* KO mice were fewer than in *Egr2* CKO mice (Fig. 4 *A–C* and Fig. S4*A*). Correspondingly, *Egr2* CKO mice had higher viral loads in their lungs than did *Egr1* KO or WT mice (Fig. 4*D*). There also was dysregulated cytokine and chemokine expression in *Egr2* CKO mice after influenza infection (Fig. S4 *B* and *C*) with sustained expression of *Il1b*, *Il6*, and *Ccl5* (Fig. S4*B*), correlating with disease severity. There also was lower expression of the Th1/Th17-related cytokine genes *Cxcl10* and *Il17a* (Fig. S4*B*), consistent with lower Th1/Th17 differentiation in vitro (Fig. 2).

Above, we observed increased lymphocytic infiltration of the lung in the *Egr2* CKO mice infected with influenza (Fig. 4*C*). Correspondingly, the number of cells in lung parenchyma was increased (Fig. S5*A*), and the frequency (Fig. S5 *B* and *C*) and absolute number (Fig. S5*C*) of TCRβ$^+$, CD4$^+$, and CD8$^+$ T cells in the lungs were higher in *Egr2* CKO mice than in *Egr1* KO or WT mice during primary infection (Fig. S5 *B* and *C*). These populations were also somewhat increased during recall responses (Fig. S5*D*, *Upper*) and sustained at high levels until day 14 postsecondary infection (Fig. S5*D*, *Lower*), whereas WT and *Egr1* KO mice had similar levels at days 8 and 14 (Fig. S5*D*). At the peak of T-cell responses to primary (PR8, day 10) and recall (X-79 then PR8, day 8) infection, the total splenocyte and CD4$^+$ and CD8$^+$ splenic T-cell numbers were similar in *Egr1* KO and

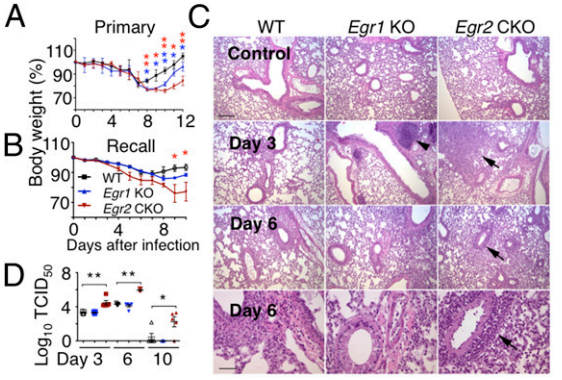

Fig. 4. *Egr2* CKO mice exhibit greater pathology than WT mice after influenza virus infection. (*A* and *B*) Body weight in WT, *Egr1* KO, or *Egr2* CKO mice in primary (*A*) and recall (*B*) infection models. (*C*) Histological examination on days 0, 3, and 6 after primary infection. (Scale bar in *Top Left*, 200 μm for the *Top* three rows; scale bar in *Lower Left*, 50 μm for the higher magnification view in the *Bottom* row.) Arrowhead, enlarged lymph node; arrows, perivascular lymphocyte infiltration. (*D*) Viral titers (50% tissue culture infectious dose, $TCID_{50}$) from lungs on days 3, 6, and 10 after primary influenza infection. Data are representative of three experiments each with five mice per group (mean ± SD) in *A* and *B*, from representative experiments in *C*, or from one of three similar experiments (mean ± SD) in *D*.

WT mice, but decreased in *Egr2* CKO mice (Fig. S5*E*), in contrast to the increased cellularity observed in their lungs. These observations indicate a key role for *Egr2* in the normal immune response to influenza.

Defective CD4$^+$ T-cell Response with Lower Cytokine Expression in *Egr2* CKO Mice After Influenza Infection. As shown above, infection with influenza virus induces T-cell proliferation (Fig. S5). However, after both primary and recall infection, similar numbers of CD4$^+$ T cells specific for the immunodominant viral nucleoprotein epitope (I-A^{b}NP$_{311–325}$, termed NP$_{311–325}$) were present in the lung (Fig. 5 *A* and *B*) and mediastinal lymph nodes (MLNs) (Fig. S6*A*) at the peak response time in *Egr2* CKO mice and WT mice. To assess the function of the antigen-specific CD4$^+$ T cells, we stimulated lung cells with NP$_{311–325}$ peptide or PMA + ionomycin. In both primary and recall infection models, we found slightly decreased frequencies of TNFα$^+$, IFN-γ$^+$, and IL-2$^+$ *Egr2* CKO CD4$^+$ T cells after stimulation with PMA + ionomycin (Fig. 5 *C*, *Upper* and *D*, *Upper*). However, significantly fewer TNFα$^+$IFN-γ$^+$CD4$^+$ T cells (Fig. 5*C*, *Lower* and Fig. S6*B*) and IL-2$^+$CD4$^+$ T cells (Fig. 5*D*, *Lower* and Fig. S6*B*) were seen in the *Egr2* CKO than in WT mice after NP$_{311–325}$ stimulation, and fewer IFN-γ, TNF, and IL-2–expressing CD4$^+$ T cells were observed in the *Egr2* CKO MLNs (Fig. S6*C*). We also identified T follicular helper (T$_{FH}$) cells from MLNs on day 10 after primary infection, based on PD-1 and CXCR5 surface markers and intracellular BCL6 expression. The frequency (Fig. S6*D*) and number (Fig. S6*E*) of PD-1$^+$CXCR5$^+$ cells were similar in WT and *Egr2* CKO mice as was the expression of BCL6 (Fig. S6 *F* and *G*) and the number of antigen-specific T$_{FH}$ cells (Fig. S6*H*).

Fewer Lung-Resident Memory CD8$^+$ T Cells in *Egr2* CKO Mice After Influenza Infection. After primary infection, although similar numbers of antigen-specific CD8$^+$ T cells were found in the MLNs from *Egr2* CKO and WT mice (Fig. S6*A*), more CD8$^+$ T cells specific for the D^{b}NP$_{366–374}$ (termed NP$_{366–374}$) were present in the lung at the peak response time in *Egr2* CKO mice (Fig. 6 *A* and *B*), and the frequency and number of NP$_{366–374}$$^+$CD8$^+$ T cells in the *Egr2* CKO were also slightly increased in the recall

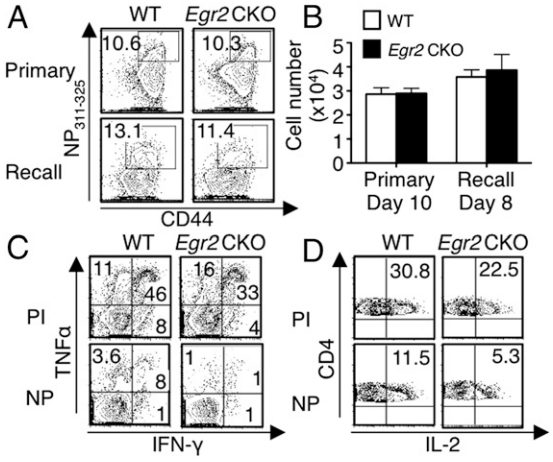

Fig. 5. IFN-γ, TNFα, and IL-2 production is lower in *Egr2* CKO CD4$^+$ than in WT CD4$^+$ T cells after influenza infection. (*A* and *B*) Lung cells were isolated and stained with NP$_{311–325}$ tetramer. Frequency (*A*) and absolute NP$_{311–325}$$^+$CD4$^+$ T-cell numbers (*B*) at the primary and recall infection peak time points. (*C* and *D*) Lung cells were stimulated with PMA + ionomycin (PI) or influenza NP peptide for 5 h, with Golgi-stop added during the last 3 h. Flow cytometric profiles for IFN-γ and TNFα (*C*), and IL-2 (*D*) expression at the peak response for primary infection. Data are from one of three experiments in *A*, *C*, and *D* or from three experiments each with five mice per group (mean ± SD) in *B*.

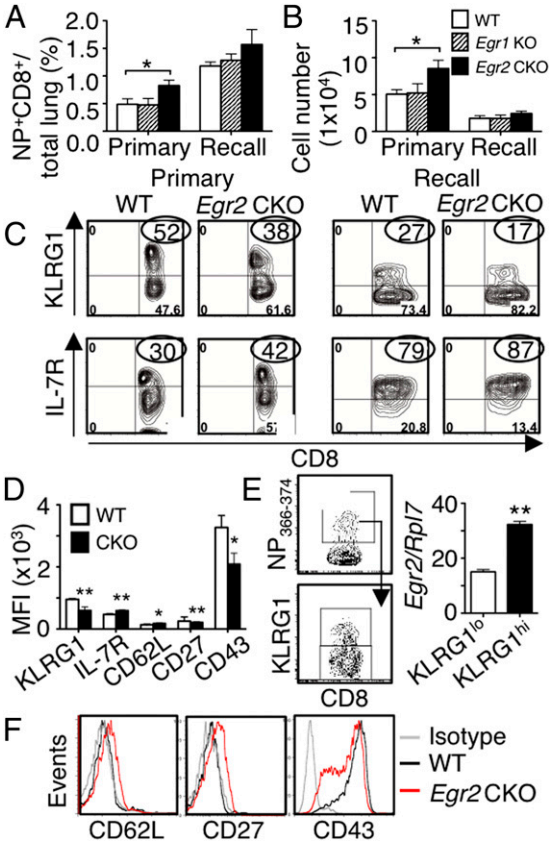

Fig. 6. A higher percentage of antigen-specific CD8$^+$ T cells have a memory phenotype in *Egr2* CKO mice than in WT mice after influenza infection. (*A* and *B*) Lung cells were stained with NP$_{366–374}$ pentamer. Frequency (*A*) and absolute NP$^+$CD8$^+$ cell numbers (*B*) at peak primary and recall infection time points. (*C*) Flow cytometric profile of KLRG1^{hi} and IL-7R^{hi} antigen-specific CD8$^+$ T cells in primary (*Left*) or recall (*Right*) infection models. (*D*) Mean fluorescent intensity (MFI) of KLRG1, IL-7R, CD62L, CD27, and CD43 from antigen-specific CD8$^+$ T cells after primary infection. (*E*) Antigen-specific KLRG1^{lo} and KLRG1^{hi} CD8$^+$ T cells were sorted and *Egr2* RNA expression on the two populations. (*F*) FACS profile of CD62L, CD27, and CD43 expression in antigen-specific CD8$^+$ T cells. Data are for 24 mice per group, combined from four experiments (mean ± SD) in *A*, *B*, and *D* or from representative experiments in *C*, *E*, and *F*.

response (Fig. 6 *A* and *B*). However, the *Egr1* KO antigen-specific CD8$^+$ T cells were similar to WT cells (Fig. 6 *A* and *B*). During infection, KLRG1^{hi}IL-7R^{lo}CD8$^+$ T effector cells lack memory potential, whereas KLRG1^{lo}IL-7R^{hi} cells are precursors for long-lived memory T cells (19). At the peaks of both primary and recall responses, in *Egr2* CKO mice, NP$_{366–374}$$^+$CD8$^+$ T cells in the lung had lower KLRG1 but higher IL-7R expression (Fig. 6 *C* and *D*) and the WT KLRG1^{hi}NP$_{366–374}$$^+$CD8$^+$ T cells expressed more *Egr2* than the WT KLRG1^{lo}NP$_{366–374}$$^+$CD8$^+$ T cells (Fig. 6*E*), consistent with the reported higher expression of EGR2 on CD44^{hi} T cells (9). Moreover, virus-specific *Egr2* CKO CD8$^+$ T cells had increased CD62L and CD27 but decreased CD43 expression (Fig. 6 *D* and *F*), a phenotype consistent with impaired effector differentiation, suggesting that EGR2 is needed for normal effector cell development.

We next measured virus-specific CD8$^+$ T cells 6 wk after primary infection and found that *Egr2* CKO mice had more NP$_{336–374}$$^+$CD8$^+$ T cells in the lung but similar numbers in the spleen and MLN, compared with WT mice (Fig. 7 *A* and *B*). However, both the total CD8$^+$ (Fig. 7*C*, *Upper*) and the antigen-specific CD8$^+$ T cells (Fig. 7*C*, *Lower*) in *Egr2* CKO mice had a lower frequency and absolute number of cells expressing

CD103 and CD69 (Fig. 7*D*), indicating fewer lung-resident memory T cells and suggesting a possible role for EGR2 in their development or accumulation.

Decreased IFN-γ and TNFα Production and CD8$^+$ Effector Function in *Egr2* CKO Mice After Influenza Infection. Analogous to the impaired IFN-γ and TNFα production by CD4$^+$ T cells, in both primary and recall infection models, significantly fewer IFN-γ and TNFα expressing CD8$^+$ T cells in *Egr2* CKO than in WT lungs (Fig. 8 *A*–*C*) and MLNs (Fig. S7*A*) in response to NP peptide stimulation. Based on the ChIP-Seq data, EGR2 bound the *Ifng* and *Tnf* loci (Fig. 8 *D* and *E*), indicating they are direct EGR2 target genes. Moreover, *Ifng* and *Tnf* expression tended to be slightly albeit not significantly lower in *Egr2* CKO than in WT cells after influenza infection (Fig. S7*B*, *Left*), whereas both *Ifng* and *Tnf* mRNA were much less potently induced in response to PMA + ionomycin in the *Egr2* CKO cells in vitro (Fig. S7*B*, *Right*). The genes encoding granzyme (*Gzmb*) and perforin (*Prf1*) each had significantly lower expression in *Egr2* CKO cells in the primary infection model and modestly decreased expression with recall infection (Fig. 8*F*), although based on ChIP-Seq, neither *Gzmb* nor *Prf1* is a direct EGR2 target gene. To identify whether the defect of the *Egr2* CKO CD8$^+$ T-cell response to influenza is intrinsic to CD8$^+$ T cells or not, we used the mouse LCMV CD8$^+$ TCR transgenic P14 system (cells specific for LCMV D^b-restricted epitope GP33-41). We cotransferred both WT (Thy1.1$^+$Thy1.2$^+$) and *Egr2* CKO (Thy1.1$^-$Thy1.2$^+$) P14 cells into CD45.1 congenic B6 mice and infected them one day later with the PR8-33 virus in which the NA gene of PR8 has the LCMV gp33-41 epitope and found a similar CD8 phenotype (Fig. S8) to that seen in the *Egr2* CKO mice. Thus, *Egr2* CKO CD8$^+$ T cells responded to influenza challenge, but the antigen-specific cells that accumulated in the lung have an increased memory precursor phenotype and decreased expression of *Ifng*, *Tnf*, *Gzmb*, and *Prf1*, underscoring an essential intrinsic role for EGR2 in the normal CD8$^+$ T-cell immune response to influenza infection.

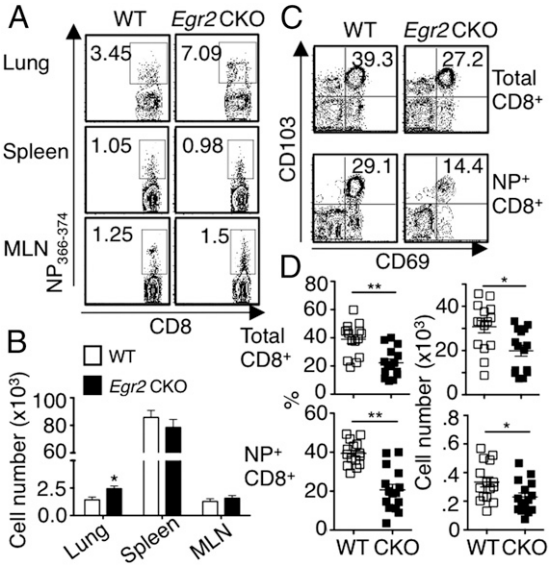

Fig. 7. Fewer CD103$^+$CD69$^+$ lung-resident memory CD8$^+$ T cells in lungs of *Egr2* CKO than in WT mice, 6 wk after influenza infection. (*A* and *B*) Cells from lung, spleen, and MLN were isolated and stained with NP$_{366–374}$ pentamer. Frequency (*A*) and absolute NP$^+$CD8$^+$ cell numbers (*B*) after 6-wk infection. (*C*) Expression of CD103 and CD69 on both total CD8$^+$ (*Upper*) and antigen-specific CD8$^+$ (*Lower*) T cells. (*D*) Frequency (*Left*) and absolute numbers (*Right*) of CD103$^+$CD69$^+$ T cells. Data are from one representative of three experiments in *A* and *C* or from three experiments each with five mice per group (mean ± SD) in *B* and *D*.

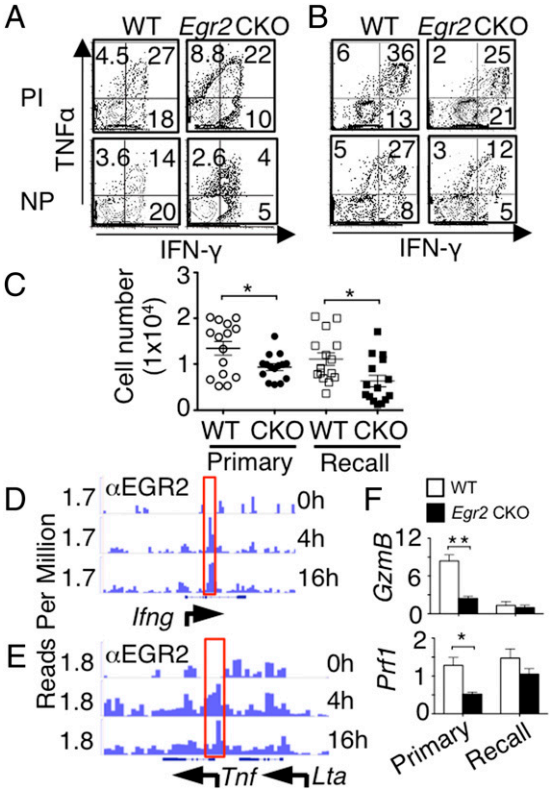

Fig. 8. IFN-γ and TNFα production and CD8 effector function are lower in *Egr2* CKO than in WT mice after influenza infection. (*A*–*C*) Lung cells were stimulated with PMA + ionomycin (PI) or influenza NP peptide for 5 h, with Golgi-stop added during the last 3 h. Representative flow cytometric profiles for TNFα and IFN-γ expression at the peak response for primary (*A*) and recall (*B*) infection models. (*C*) Absolute number of TNFα$^+$IFN-γ$^+$CD8$^+$ T cells with NP peptide stimulation. (*D* and *E*) ChIP-Seq analysis of the EGR2 binding at the *Ifng* (*D*) and *Tnf* (*E*) loci. (*F*) mRNA expression (RT-PCR) of *Gzmb* and *Prf1* in CD8$^+$ T cells purified after primary or recall infection models. Data are from one representative of three experiments in *A* and *B*, from three experiments with 15 mice combined (mean ± SD) in *C*, representative of two independent experiments in *D* and *E* or from three experiments each with five mice per group (*F*).

Discussion

Using *CD4*-Cre *Egr2* CKO mice, we have shown that EGR2 is required for normal T-cell proliferation and differentiation under both normal and pathological conditions. *Egr2* deficiency resulted in delayed TCR-induced proliferation of naïve CD4$^+$ and CD8$^+$ T cells, at least in part due to defective IL-2 production, and EGR2 was also required for normal Th1, Th2, Th9, Th17, and Tc cell differentiation and cytokine production. After influenza virus infection, *Egr2* CKO mice exhibited prolonged viral shedding, increased weight loss, impaired CD4$^+$ T-cell response with decreased IFN-γ and TNFα, increased infiltration into the lung of memory precursor type CD8$^+$ T cells with decreased expression of granzyme B and perforin as well as diminished IFN-γ and TNFα. In contrast, *Egr1* KO T cells had only slightly defective proliferation and differentiation, with slightly decreased production of IFN-γ and IL-4, with similar survival and immune responses in influenza-infected *Egr1* KO mice and WT mice.

Analysis of *Egr2* CKO mice revealed significantly decreased CD4$^+$ and CD8$^+$ T cells in both lymph node and spleen, consistent with a role for EGR2 in development. Interestingly, in

this regard, EGR2 was reported to regulate BCL2 expression during positive selection (20). Consistent with a positive role of EGR2 in naïve T-cell proliferation and differentiation, there was decreased expression of a number of genes, 36 of which bound EGR2, including *Tbx21* and *Notch1*. We also identified a number of transcription factors that promote T-cell activation and differentiation and have diminished expression in *Egr2* CKO T cells, but which appear to be indirectly regulated by EGR2. The reasons for the unexpectedly lower production of TCR-induced IFN-γ and IL-17A in our *Egr2* CKO $CD4^+$ T cells, which contrasts to the increased expression in *CD2-Egr2* CKO or *CD2-Egr2Egr3* DKO mice (9, 11) are unclear but could reflect different microenvironments in T-cell development in vivo due to *Egr2* gene knockout at different stages (DN for CD2-Cre versus DP for CD4-Cre).

A previous study reported that *Egr2* CKO mice can mount normal in vivo T-cell responses to infection with *T. gondii* or LCMV (13). Here, we now show that EGR2 is required for a normal immune response to influenza infection, with greater weight loss and more severe pathological changes, as well as sustained viral shedding in the lung until day 10 in *Egr2* CKO mice. Consistent with this robust viral shedding, *Egr2* deficiency led to a significant increase in the frequency and total number of $CD4^+$ and $CD8^+$ T cells in the lungs, and this was sustained for greater than 2 wk after the resolution of infection. Decreased $CD4^+$ and $CD8^+$ T cells in spleens of *Egr2* CKO mice at the peaks of primary and recall infection suggests either altered trafficking to the infection site or dysregulated T-cell production in the spleen. The increased antigen-specific $CD8^+$ T cells in the lungs confirmed that EGR2 affects T-cell accumulation, and the infiltration of impaired $CD4^+$ T cells with diminished cytokines and memory precursor phenotype $CD8^+$ T cells with impaired function and dysregulated cytokine may explain the delayed viral clearance and prolonged $CD8^+$ T-cell infiltration in *Egr2* CKO mice. Previous studies have shown important functions for *Notch1* and *Tbx21*-dependent pathways in influenza infection for normal antigen-specific $CD8^+$ T-cell immune responses (21, 22) and cytokine/chemokine expression (23). The regulation of *Notch1* and *Tbx21* by EGR2 thus helps to explain the importance of EGR2 for a normal immune response to influenza.

Overall, our data demonstrate that EGR2 promotes naïve T-cell proliferation and differentiation both in vitro in response to TCR stimulation and in vivo after influenza virus infection. In addition to previously reported negative regulatory roles for EGR2, our data reveal that EGR2 can also exert positive regulatory effects, indicating that EGR2 may represent a new target for the control of influenza virus.

Materials and Methods

Mice. See *SI Materials and Methods*.

Th Polarization. Th1, Th2, Th9, Th17, and Tc cell differentiation were performed as previously reported (24). See *SI Materials and Methods*.

RNA-Seq and ChIP-Seq. RNA-Seq and ChIP-Seq were performed as previously reported (18, 24). See *SI Materials and Methods*.

Viral Infection. See *SI Materials and Methods*.

Cell Transfers. The same number of WT and CKO P14 cells (2.5×10^4 each) was transferred into $Thy1.1^+$ (B6. PL-$Thy1^a$/CyJ) mice by i.p. One day later, mice were infected with 10^3 50% egg infectious dose (EID_{50}) of PR8-33.

Flow Cytometry. Surface and intracellular staining were performed per the standard protocol. See *SI Materials and Methods*.

Statistical Analysis. One-way analysis of variance or two-tailed paired *t* tests were performed using Prism 4.0 (GraphPad software). Statistical significance is indicated by $*P < 0.05$, $**P < 0.01$. Shown is mean ± SD.

ACKNOWLEDGMENTS. We thank J.-X. Lin and R. Spolski (NHLBI) for critical comments, S. Epstein (Food and Drug Administration) for PR8 and X-79 strains of influenza virus, J. Zhu and Y. Wakabayashi (NHLBI DNA Sequencing Core) for excellent services, and NHLBI Flow Cytometry Core Facility for cell sorting and sample analysis. This work was supported by the Division of Intramural Research, National Heart, Lung, and Blood Institute (NHLBI), National Institutes of Health.

1. Dias S, Xu W, McGregor S, Kee B (2008) Transcriptional regulation of lymphocyte development. *Curr Opin Genet Dev* 18(5):441–448.
2. Carleton M, et al. (2002) Early growth response transcription factors are required for development of CD4(-)CD8(-) thymocytes to the CD4(+)CD8(+) stage. *J Immunol* 168(4):1649–1658.
3. Bettini M, Xi H, Milbrandt J, Kersh GJ (2002) Thymocyte development in early growth response gene 1-deficient mice. *J Immunol* 169(4):1713–1720.
4. Topilko P, et al. (1994) Krox-20 controls myelination in the peripheral nervous system. *Nature* 371(6500):796–799.
5. Li S, et al. (2011) Early growth response gene-2 (Egr-2) regulates the development of B and T cells. *PLoS One* 6(4):e18498.
6. Rengarajan J, et al. (2000) Sequential involvement of NFAT and Egr transcription factors in FasL regulation. *Immunity* 12(3):293–300.
7. Safford M, et al. (2005) Egr-2 and Egr-3 are negative regulators of T cell activation. *Nat Immunol* 6(5):472–480.
8. Zheng Y, Zha Y, Driessens G, Locke F, Gajewski TF (2012) Transcriptional regulator early growth response gene 2 (Egr2) is required for T cell anergy in vitro and in vivo. *J Exp Med* 209(12):2157–2163.
9. Zhu B, et al. (2008) Early growth response gene 2 (Egr-2) controls the self-tolerance of T cells and prevents the development of lupuslike autoimmune disease. *J Exp Med* 205(10):2295–2307.
10. Miao T, et al. (2013) Early growth response gene-2 controls IL-17 expression and Th17 differentiation by negatively regulating Batf. *J Immunol* 190(1):58–65.
11. Li S, et al. (2012) The transcription factors Egr2 and Egr3 are essential for the control of inflammation and antigen-induced proliferation of B and T cells. *Immunity* 37(4):685–696.
12. Lee SL, Tourtellotte LC, Wesselschmidt RL, Milbrandt J (1995) Growth and differentiation proceeds normally in cells deficient in the immediate early gene NGFI-A. *J Biol Chem* 270(17):9971–9977.
13. Ramón HE, et al. (2010) EGR-2 is not required for in vivo CD4 T cell mediated immune responses. *PLoS ONE* 5(9):e12904.
14. Shin HJ, Lee JB, Park SH, Chang J, Lee CW (2009) T-bet expression is regulated by EGR1-mediated signaling in activated T cells. *Clin Immunol* 131(3):385–394.
15. Auderset F, Coutaz M, Tacchini-Cottier F (2012) The role of Notch in the differentiation of $CD4^+$ T helper cells. *Curr Top Microbiol Immunol* 360:115–134.
16. Lin JX, Leonard WJ (2000) The role of Stat5a and Stat5b in signaling by IL-2 family cytokines. *Oncogene* 19(21):2566–2576.
17. Yagi R, Zhu J, Paul WE (2011) An updated view on transcription factor GATA3-mediated regulation of Th1 and Th2 cell differentiation. *Int Immunol* 23(7):415–420.
18. Lin JX, et al. (2012) Critical role of STAT5 transcription factor tetramerization for cytokine responses and normal immune function. *Immunity* 36(4):586–599.
19. Joshi NS, et al. (2007) Inflammation directs memory precursor and short-lived effector CD8(+) T cell fates via the graded expression of T-bet transcription factor. *Immunity* 27(2):281–295.
20. Lauritsen JP, et al. (2008) Egr2 is required for Bcl-2 induction during positive selection. *J Immunol* 181(11):7778–7785.
21. Kuijk LM, et al. (2013) Notch controls generation and function of human effector CD8+ T cells. *Blood* 121(14):2638–2646.
22. Ito T, et al. (2011) The critical role of Notch ligand Delta-like 1 in the pathogenesis of influenza A virus (H1N1) infection. *PLoS Pathog* 7(11):e1002341.
23. Dutta A, et al. (2013) Altered T-bet dominance in IFN-γ-decoupled CD4+ T cells with attenuated cytokine storm and preserved memory in influenza. *J Immunol* 190(8):4205–4214.
24. Liao W, Lin JX, Wang L, Li P, Leonard WJ (2011) Modulation of cytokine receptors by IL-2 broadly regulates differentiation into helper T cell lineages. *Nat Immunol* 12(6):551–559.